

# Vehicle-to-Infrastructure Communications Design in Urban Hyperfractals

Dalia Popescu  
Nokia Bell Labs  
France

dalia-georgiana.popescu@nokia-bell-labs.com

Philippe Jacquet  
Nokia Bell Labs  
France

philippe.jacquet@nokia-bell-labs.com

**Abstract**—The goal of this study is to increase the awareness about the communication opportunities that arise in urban vehicle networks when exploiting the self-similarity and hierarchical organization of modern cities. The work uses our innovative model called “hyperfractal” that captures the self-similarity of the urban vehicular networks as well as incorporating road-side infrastructure with its own self-similarity.

We use analytical tools to provide achievable trade-offs in operating the road-side units under the constraint of minimum routing path delay while maintaining a reasonably balanced load.

The models and results are supported by simulations with different city hyperfractal dimensions in two different routing scenarios: nearest neighbor routing with no collision and minimum delay routing model assuming slotted Aloha, signal to interference ratio (SIR) capture condition, power-path loss, Rayleigh fading.

## I. INTRODUCTION

Vehicular networks have made significant progress with the daring emergence of the Internet of Things (IoT). The driverless car initiatives push towards the development of vehicular communication in all of its variants: vehicle-to-vehicle (V2V), vehicle-to-infrastructure (V2I) and vehicle-to-everything (V2X). In an intelligent transportation system (ITS), V2I sensors also called road-side units (RSU) can capture infrastructure data and provide travelers with real-time advices about road conditions, traffic congestion, accidents, construction zones, parking availability, etc [1]. Nevertheless, one of the key functionalities of the infrastructure is assisting in the vehicular communications. Such V2I sensors can include overhead RFID readers and cameras, traffic lights, lane markers, streetlights, signage and parking meters. Considerations have been made for dedicated infrastructure, yet a more economic sensible way of assisting the vehicular communications is to exploit the already existing telecommunications and traffic poles. The design of the topology of the RSU is consequently closely tied to the deployment of the vehicular communications and the vehicular traffic.

Vehicles are deployed where human activity occurs and therefore, the modeling of vehicular networks should be done accordingly, following the structural and hierarchical organization of human society. Central Place Theory (CPT) assumes the existence of regular spatial patterns in regional human organization [2]. Similarly, cities reflect a statistical self-similarity or hierarchy of clusters [3].

In mathematics, a self-similar object, or fractal, is an object which shows strong similarity with smaller parts of itself. Fractals are objects that commonly exhibit similar patterns at increasingly small scales and usually describe and simulate objects occurring in nature (see the seminal work of Mandelbrot, e.g. [4]). Fractals have been recently introduced for wireless network topology modeling as they provide a realistic description of geometric properties and interactions that arise in an urban ad hoc wireless network [5], [6].

In that sense, the aim of this paper is to provide a robust topology model based on self-similarity for V2V and V2I vehicular communications, together with the insights of operating the topology for the optimization of communication delay or infrastructure cost.

Indeed, literature shows that insights from nature can be used for intelligent network design [7]. Routing costs and energy consumption are directly dependent of the adjacent topology design as described in [8], [9]. Topology of ad hoc networks, either sensors, either cars is also relevant for anomaly detection [10], further motivating the need for an accurate, realistic modeling of V2V and V2I topologies. In [11], the authors show the impact of the topology of the RSU on the quality of the vehicular communications. The self-similarity of urban traffic in time has been proven by data fitting in [12], [13]. These works support the adequacy of self-similar processes in modeling road traffic time series over various time scales.

Exploiting the self-similarity of the urban architecture for the modeling of the vehicular communications has been recently introduced in our previous works [6], [14]–[16] where we introduced “hyperfractals” for modeling vehicular density in towns.

In this paper we extend the “hyperfractal” model that we have introduced in [6], [14] in order to better capture the impact of the network topology on the fundamental performance limits of end-to-end communications over vehicular networks in urban settings. The model consists into assigning decaying traffic densities to city streets, thus avoiding the extremes of regularity (e.g. Manhattan grid) and of uniform randomness (e.g. Poisson point process).

Our previous result in [6] showed that, for nodes, the number of hops in a routing path between an arbitrary source-destination pair increases as a power function of the population

$n$  of nodes when  $n$  tends to infinity. However, we showed that the exponent tends to zero when the hyperfractal dimension tends to infinity. Furthermore, in [15] we show how the model fits traffic data of real cities.

## II. SYSTEM MODEL

### A. Hyperfractals

For the sake of completeness, we briefly remind the reader the hyperfractal model and its key properties. For a comprehensive description, the reader is referred to [6], [14], [16] for static settings with road-side infrastructure and to [15] for mobile settings without road-side infrastructure.

The map model lays in the unit square. The support measure of the population is a grid of streets with an infinite resolution (in practice, the resolution will be limited). An example is displayed in Figure 1a. For the first level denoted as level 0, the lines are drawn in thick black. Each of the four quadrants obtained when drawing the first level lines are considered as an independent map. The process is further continued in a similar manner, inside each of the quadrants, the lines of level 1 are drawn in thinner black and so on. The thickness of the lines decreases with the level index.

### B. Hyperfractal Mobile Node Distribution

The map contains  $n$  mobile nodes. The process of assigning them to the lines is performed recursively, similar to the process of obtaining the Cantor Dust [4].

The two lines of level 0 form a central cross which splits the map in exactly 4 quadrants. We denote by probability  $p$  the probability that the mobile node is located on the cross according to a uniform distribution and  $q$  the complementary probability. With probability  $q/4$ , the mobile is located in one the four quadrants. The association procedure continues in each quadrant. A cross of level  $H$  consists of two intersecting segments of lines of level  $H$  and each segment of the cross is considered to be a segment of level  $H$ . Two segments that belong to the same line are necessarily of the same level. A street of level  $H$  consists of the union of consecutive segments of level  $H$  in the same line. The length of a street is the length of the side of the map.

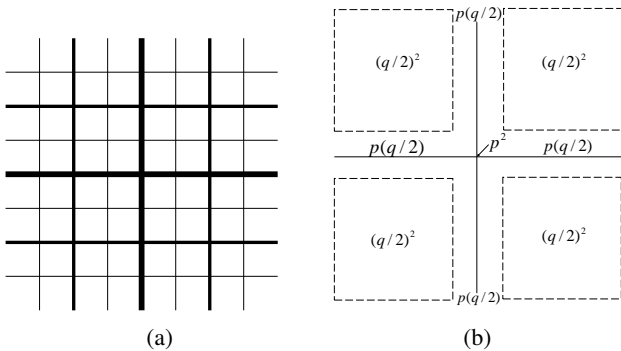


Figure 1: a) Hyperfractal map support b) Procedure of assigning relays to intersections

The density of mobile nodes in a quadrant is  $q/4$ . Let  $\lambda_H$  be the density of mobile nodes assigned on a street of level  $H$ :

$$\lambda_H = (p/2)(q/2)^H$$

In order to compute the fractal dimension, let us make use of the same reasoning as for computing the fractal dimension of Sierpinski's triangle [17]. Notice that the measure (in the Lebesgue sense), which represents the actual density of mobile nodes in the map has strong scaling properties. The map as a whole is identically reproduced in each of the four quadrants but with a weight of  $q/4$  instead of 1. Thus the measure has a structure which recalls the structure of a fractal set, such as the Cantor map [4]. A crucial difference lies in the fact that the fractal dimension here,  $d_m$ , is in fact *greater* than 2, the Euclidean dimension. Indeed, considering the map in only half of its length consists into considering the same map but with a reduced weight by a factor  $q/4$ . One obtains:

$$\left(\frac{1}{2}\right)^{d_m} = q/4, \quad \text{thus} \quad d_m = \frac{\log(\frac{4}{q})}{\log 2} > 2$$

The fractal dimension here,  $d_m$ , is in fact *greater* than 2, the Euclidean dimension. This property can only be explained via the concept of measure. Formally, the hyperfractal model is a Poisson shot model with support a measure which has some specific scaling properties.

### C. Canyon Effect

The analyzed network model incorporates a typical urban radio propagation phenomenon: the canyon effect.

The *canyon* propagation model implies that the signal emitted by a mobile node propagates only on the axis where it stands on. In [18] it is shown that the non line of sight received signal strength is very weak due to buildings and other road-side obstacles. Furthermore, [19] shows that intersections have specific propagation characteristics that can favor or not the radio propagation.

### D. Relays

Not surprisingly, locations of communication infrastructure in urban settings also display self-similar behavior. Hence we apply another hyperfractal process for selecting the intersections where a road-side relay is installed or the existing traffic light is used as RSU. This process has been introduced for the first time in [6]. For the sake of completeness, we review the model and its basic properties which will be exploited in the development of our main results.

The procedure of assigning relays to intersections is intuitively illustrated in Figure 1b. Denote by  $p'$  a fixed probability and  $q' = 1 - p'$  the complementary probability. With probability  $p'$ , an intersection holds a relay. With probability  $(p')^2$ , the selection is the central crossing of the two streets of level 0. With probability  $(p')(q'/2)$ , the relay is placed in one of the four street segments of level 0, and the process continues on the segment. Otherwise, with probability  $(q'/2)^2$ , the relay is placed in one of the four quadrants delimited by the central cross and the process continues recursively.

The placement process is performed  $M$  times. The probability that an intersection between two streets of respective levels  $H$  and  $V$  is selected to hold a relay is  $p(H, V)$ :

$$p(H, V) = (p')^2 \left( \frac{q'}{2} \right)^{H+V}.$$

If one crossing is selected multiple times, only one relay is installed in the respective crossing. To simplify the analysis and to make the intersections independent of the number of runs,  $M$  is set to be a Poisson variable of mean  $\rho$ . Consequently, an intersection of type  $(H, V)$  has the probability  $\exp(-\rho p(H, V))$  of not holding a relay and events relative to each intersection are independent.

Some basics results are further reviewed. The relay placement is hyperfractal with dimension  $d_r$ :

$$d_r = 2 \frac{\log(2/q')}{\log 2}.$$

The total number of relays in the map is:

$$R(\rho) = O(\rho^{2/d_r} \log \rho)$$

It is considered that  $\rho = \rho_n$  as a function of  $n$ , and, for the sake of simplicity,  $\rho_n = n$ . In this case, one can notice that the number of relays is, indeed, substantially smaller than the number of mobile nodes.

A complete hyperfractal map with mobile nodes and relays is illustrated in Figure 2.

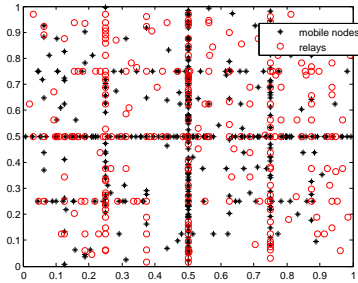


Figure 2: Complete hyperfractal map with mobiles and relays

### E. Routing

This work does not consider detailed aspects of the communication protocol. The nodes in the network, both mobile nodes and relays, communicate like in a mobile ad hoc network where packets are routed forward from their sources to their destinations. We consider a table-driven routing where each node looks into a routing table to determine the next hop to send the packet to.

The routing table is computed according to a minimum-cost path over a cost matrix  $[t_{ij}]$  where  $t_{ij}$  represents the cost of directly transmitting a packet from node  $i$  to node  $j$ . The minimum cost path from node  $i$  to node  $j$  which optimizes the relaying nodes (either mobile nodes or fixed relays) is denoted  $m_{ij}$  and satisfies:

$$m_{ij} = \min_k \{m_{ik} + t_{kj}\}, \forall(i, j).$$

Due to the canyon effect, some nodes can be disconnected. We restrict our analysis to the giant component of the network which contains the central node  $[\frac{1}{2}, \frac{1}{2}]$ . It has been shown [14] that the size of this giant component (in what regards number of mobile nodes) is strictly of order  $n$ .

In this paper two routing strategies are considered:

- the nearest neighbor routing (NN);
- the minimum delay routing.

1) *The nearest neighbor routing*: In this strategy the next hop is always a next neighbor on an axis. Thus

$$\begin{cases} t_{ij} = 1, & \text{if nodes } i \text{ and } j \text{ are aligned,} \\ & \text{and } \nexists k \text{ such that } d(i, j) = d(i, k) + d(k, j), \\ t_{ij} = \infty & \text{otherwise.} \end{cases}$$

Notice that a mobile node has at most two neighbors while a relay has at most four.

2) *The minimum delay routing*: In this model, the underlying medium access control is slotted Aloha with per-slot and per-node transmission probability  $p_A$ . Considering interference, required SIR, and attenuation factors, we denote  $p_{ij}$  the probability that node  $j$  correctly receives a packet from node  $i$  at a given slot. Clearly,  $p_{ij} \leq p_A(1 - p_A)$ , since a required condition is that node  $i$  transmits and node  $j$  does not. Therefore, the average delay required for node  $i$  to successfully transmit a packet to node  $j$  is  $t_{ij} = 1/p_{ij}$ . The quantity  $m_{ij}$  becomes the cost of the minimum average path delay.

## III. THEORETICAL RESULTS

Note that, from now on, we use the term node to refer both mobile nodes and relays.

**Definition 1.** *The load  $\gamma(x)$  of a node  $x$  is the number of paths that are routed through the respective node.*

We do not provide analytically a routing technique such that the load is balanced. Instead, we compute here the load of forwarding nodes under the constraint of minimum path cost routing (either NN, or minimum delay).

While the routing strategy is suboptimal in which regards the load balancing, we choose it as the reference routing technique in order to give insights on the load achieved when minimizing the cost. Furthermore, a minimum delay routing technique is of interest as it maximizes the network throughput.

In our previous work, [6], the average path cost both for NN routing and for minimum delay routing,  $D_n$  was derived under the constraint of minimum cost as:

$$D_n = O\left(n^{1 - \frac{2}{(1+1/d_m)^{d_r}}}\right) \quad (1)$$

In the hyperfractal, there are a total of  $L_n = |G| * (|G| - 1)$  routes between the nodes, where  $|G|$  is the size of the giant component. It has been previously shown [14] that the giant component,  $G$ , tends to include all the nodes in the network.

Throughout the derivations, we make the simplistic assumption that all nodes have equal traffic toward all destinations and

each node  $x$  has the same capacity  $C(x) = C$  and supports a load  $\gamma(x)$  as per Definition 1.

We further define the following quantities:  $\mu_n$  as the capacity per route per node,  $C_n$  the total capacity of routes.

**Remark 1.** *The aggregate throughput of routes that pass through a node is inferior to the capacity of the node.*

$$\mu_n \gamma(x) \leq C(x) \quad (2)$$

Under these assumptions and observations, the following hold:

**Theorem 1.** *The aggregate throughput of routes multiplied by the length of routes is inferior to the sum of the capacity of all the nodes.*

$$L_n C_n \leq \sum_{x \in G} C(x)$$

*Proof.* The average load of the nodes in a hyperfractal is:

$$\mathbb{E}[\gamma(x)] = \frac{D_n L_n}{n + R(\rho)} \quad (3)$$

Substituting in (2) and multiplying on both sides with  $|G| = n + R(\rho)$ :

$$\mu_n D_n L_n \leq \sum_{x \in G} C(x)$$

As the capacity of the routes is  $C_n = \mu_n D_n$  we arrive to the result that we write as:

$$\mu_n D_n L_n (1 + \epsilon) = |G| C$$

with  $1 + \epsilon$  a positive number.  $\square$

A lower bound on the capacity of the network can be derived. The minimum capacity of a route is achieved by minimizing:

$$\mu_{min} = \min_{x \in G} \left( \frac{C}{\gamma(x)} \right)$$

Replacing  $\mu_n$  by using (2), the minimum will be obtained as:

$$\min \left( \frac{1}{\gamma(x)} \right) = \frac{n + R(\rho)}{D_n L_n (1 + \epsilon)} \quad (4)$$

Denote by  $\Gamma = \max_{x \in G} (\gamma(x))$  the maximum achieved load in the hyperfractal network. As it strongly depends on the employed routing technique,  $\Gamma$  is a quantity that can be determined only empirically.

**Definition 2.** *We define by  $\tau = 1 + \epsilon$  as the peak to average load ratio.*

By (3) and (4):

$$\tau = \frac{\Gamma}{\mathbb{E}[\gamma]} \quad (5)$$

This quantity shows whether the load is balanced in the network. A high peak-to-average load ratio implies the existence a bottleneck, a node that is charged with routing considerably more routes than the other nodes in the network and that can represent a point of failure. Being a function of  $\Gamma$ , the value of  $\tau$  is determined through simulations.

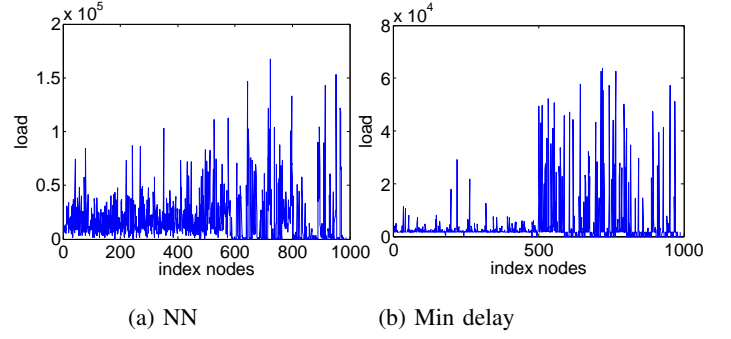


Figure 3: Load distribution in hyperfractal  $d_m = 3.3$ ,  $d_r = 2.3$ , nodes index up to index 500, relays index starting from index 500

The lower bound on capacity is therefore achieved for the bottleneck:

$$\mu_{min} = \frac{C}{\Gamma}$$

Consequently,

**Corollary 1.1.** *The network capacity in a hyperfractal is higher than:*

$$C_n \geq \frac{C}{\Gamma} |G| (|G| - 1)$$

where  $\Gamma$  is the maximum load achieved in the network.

This corollary shows that the network capacity is limited by the bottleneck of the network, therefore, a routing technique that provides a low peak to average load can be beneficial for the network capacity.

#### IV. SIMULATIONS

This section presents simulations in a two dimensional network which follows the model presented in Section II. The simulations are performed by using both routing strategies.

For the minimum delay routing, it is assumed that each transmitting node uses the same nominal transmit power and that the received signal is affected by path-loss  $l(i, j)$  and Rayleigh fading.

The following results are used for computing the probabilities of successful reception,  $p_{ij}$  when independent Rayleigh fading is applied [6]:

$$p_{ij} = p_A (1 - p_A) \prod_{k \neq i, j} w_{kj} (K/l(i, j)).$$

where  $w_{kj}(\theta)$  is the Laplace transform of the pdf of the signal produced by node  $k$  over node  $j$ ,  $p_A$  is the Aloha medium access probability, and  $K$  is the Signal to Interference Ratio (SIR). In the following, the pathloss coefficient  $\alpha = 4$  and  $K = 1$ .

The validations are performed for several configurations with different values of  $n$ ,  $d_m$  and  $d_r$ .

Figures 3a showcases the distribution of load for a hyperfractal configuration  $d_m = 3.2$ ,  $d_r = 2.3$  for the nearest node routing strategy. The indexes of the relays start after the index

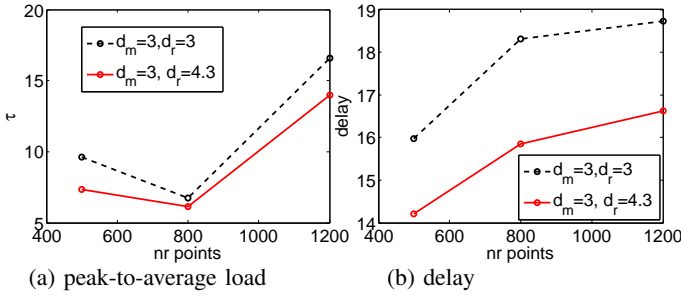


Figure 4: Peak-to-average load (a) and delay (b) for two configurations, NN routing

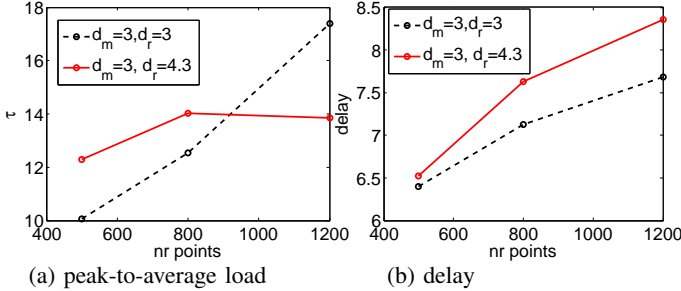


Figure 5: Peak-to-average load (a) and delay (b) for two configurations, min delay routing

500. Notice that the relays support loads of routes that are superior to the load supported by the mobile nodes, with a easily distinguishable maximum.

When using the minimum delay routing strategy, the load distribution changes dramatically, see Figure 3b. For the same hyperfractal configuration,  $d_m = 3.2$ ,  $d_r = 2.3$ , the relays are heavily loaded, while the mobile nodes support a much lighter traffic.

Let us look now to the peak-to-average load,  $\tau$ , and the delay in two configurations. Figure 4a shows the peak-to-average load for different values of  $n$  in two configurations, with the same fractal dimension of mobile nodes,  $d_m = 3$ , but different value for the fractal dimension of relays,  $d_r = 3$  in the first configuration, and  $d_r = 4.3$  in the second one. One can easily notice that the load is better balanced when the fractal dimension of relays is higher. Figure 4b confirms that the second configuration outperforms the first configuration as the delay achieved in the second configuration is inferior to the delay achieved when  $d_r = 4.3$ .

For the minimum delay routing technique, Figure 5a shows the peak-to-average load for different values of  $n$  in two configurations, with the same fractal dimension of mobile nodes,  $d_m = 3$ , but different values for the fractal dimension of relays,  $d_r = 3$  and  $d_r = 4.3$ , respectively. In this case, the first configuration offers a lower delay, yet the bottleneck of the network with the increase of nodes evolves better for the second configuration. This suggests that the choice of the fractal dimension of the infrastructure has to be done accordingly, with respect to the quality of service constraints

and allowed trade-offs.

## V. CONCLUSIONS

This work has presented and extended the hyperfractal model for vehicular networks with an emphasis on the infrastructure topology.

We provided here insights on the operating characteristics of the V2I networks, more precisely on the peak-to-average load of the nodes when a minimum cost routing technique is imposed. A consequence of the main result is a lower bound on the network capacity.

Further work will focus into data fitting for the relay hyperfractal model for further advocating the validity of the model.

## REFERENCES

- [1] "What is vehicle to infrastructure?" <http://whatis.techtarget.com/definition/vehicle-to-infrastructure-V2I-or-V2X>.
- [2] S. Grauwil, M. Szell, S. Sobolevsky, P. Hvel, and F. Simini, "Identifying and modeling the structural discontinuities of human interactions," *Nature Scientific Reports*, vol. 7, no. 46677, 2017.
- [3] M. Batty, "The size, scale, and shape of cities," *Science*, 2008.
- [4] B. B. Mandelbrot, *The Fractal Geometry of Nature*, 1983.
- [5] P. Jacquet, "Optimized outage capacity in random wireless networks in uniform and fractal maps," in *ISIT*, June 2015, pp. 166–170.
- [6] P. Jacquet and D. Popescu, "Self-similarity in urban wireless networks: Hyperfractals," in *Workshop on Spatial Stochastic Models for Wireless Networks, SpaSWiN*, May 2017.
- [7] S. Toumpis, "Mother nature knows best: A survey of recent results on wireless networks based on analogies with physics," *Computer Networks*.
- [8] A. Crismani, U. Schilcher, S. Toumpis, G. Brandner, and C. Bettstetter, "Packet travel times in wireless relay chains under spatially and temporally dependent interference," in *2014 ICC*, June.
- [9] J. Zhu and S. Papavassiliou, "On the energy-efficient organization and the lifetime of multi-hop sensor networks," *IEEE Communications Letters*, Nov.
- [10] V. Chatzigiannakis, S. Papavassiliou, M. Grammatikou, and B. Maglaris, "Hierarchical anomaly detection in distributed large-scale sensor networks," in *ISCC'06*, June.
- [11] V. Shivaldova, M. Sepulcre, A. Winkelbauer, J. Gozalvez, and C. F. Mecklenbrauker, "A model for vehicle-to-infrastructure communications in urban environments," in *2015 ICCW*, June.
- [12] G. S. Thakur, P. Hui, and A. Helmy, "On the existence of self-similarity in large-scale vehicular networks," in *2013 9th International Wireless Communications and Mobile Computing Conference (IWCMC)*, July.
- [13] "Traffic analysis of vehicular ad-hoc networks of v2i communication," *Procedia Computer Science*, eleventh International Conference on Communication Networks, ICCN 2015, August 21-23, 2015.
- [14] P. Jacquet and D. Popescu, "Self-similar Geometry for Ad-Hoc Wireless Networks: Hyperfractals," in *3rd conference on Geometric Science of Information*.
- [15] P. Jacquet, D. Popescu, and B. Mans, "Information dissemination in vehicular networks in an urban hyperfractal topology," <http://arxiv.org/abs/1712.04054>.
- [16] —, "Energy Trade-offs for end-to-end Communications in Urban Vehicular Networks exploiting an Hyperfractal Model," Jan. 2018, working paper or preprint.
- [17] W. contributors, "Sierpinski triangle — wikipedia, the free encyclopedia," 2018, [Online; accessed 1-February-2018]. [Online]. Available: [https://en.wikipedia.org/w/index.php?title=Sierpinski\\_triangle&oldid=820536727](https://en.wikipedia.org/w/index.php?title=Sierpinski_triangle&oldid=820536727)
- [18] B. Aygun, M. Boban, J. P. Vilela, and A. M. Wyglinski, "Geometry-based propagation modeling and simulation of vehicle-to-infrastructure links," in *2016 VTC Spring*, May.
- [19] J. Karedal, F. Tufvesson, T. Abbas, O. Klemp, A. Paier, L. Bernado, and A. F. Molisch, "Radio channel measurements at street intersections for vehicle-to-vehicle safety applications," in *2010 VTC*, May.